Journal of Structural Geology, Vol. 12, No. 5/6, pp. 651 to 665, 1990
Printed in Great Britain

0191-8141/90 $03.00+0.00

The geological evolution of the Reynolds Range, central Australia: evidence for three distinct structural–metamorphic cycles

PAUL H. G. M. DIRKS and CHRISTOPHER J. L. WILSON

Department of Geology, University of Melbourne, Parkville, Victoria 3052, Australia

(*Received* 10 *February* 1989; *accepted in revised form* 15 *January* 1990)

Abstract—The Reynolds Range is affected by three distinct structural–metamorphic cycles, *D*I–*M*I, *D*II–*M*II and *D*III–*M*III, which represent the local expressions of a series of orogenic events that affected large sections of the Arunta Block, central Australia. The tectonic cycles recognized in the Reynolds Range correlate extremely well with similar events in the nearby Anmatjira Range. *D*I–*M*I took place around 1820 Ma and only affected the NW Reynolds Range. *D*II–*M*II occurred between 1760 and 1650 Ma and involved NE–SW shortening with identical timing relationships between the deformations and metamorphism along the entire Reynolds Range. *D*II commenced with the formation of a fabric, SII_1, preserved as inclusion trails in porphyroblasts. SII_1 formed early during a progressive event, DII_{1-2}, which involved the formation and tightening of upright NW–SE-trending isoclinal folds. A penetrative subvertical NW–SE-trending fabric, SII_2, developed axial planar to these folds. The general symmetry of DII_2 microstructures suggests that FII_2 folds were formed during progressive coaxial deformation under plane strain conditions. DII_3 structures are associated with conjugate sets of crenulation bands. Within the macroscopic crenulation bands, large sections of earlier folds and fabrics are rotated to a near recumbent position. The dominant set of crenulation bands is upright and trends ENE–WSW while the conjugate to this set trends NW–SE. No penetrative fabric formed during DII_3. DII_4 is associated with a system of amphibolite-grade NE-dipping thrusts interconnected by numerous smaller shear zones. The sense of movement is NE-over-SW. During *D*II essentially penetrative coaxial deformation (DII_2) evolved into essentially localized non-coaxial deformation (DII_3–DII_4).

*D*II deformation occurred concomitant with a low-pressure granulite-facies metamorphic event (*M*II, 1730 Ma). Peak metamorphic sillimanite + cordierite + orthopyroxene + ilmenite + spinel + garnet + K-feldspar + quartz assemblages define SII_2. Oriented sillimanite + biotite assemblages that formed early during DII_3 and unoriented andalusite + chlorite + muscovite assemblages that formed late during DII_3 indicate that cooling of *M*II was initially isobaric. During DII_4 thrusting staurolite + garnet + biotite + quartz and biotite + kyanite + quartz assemblages, defining the mylonitic fabric, overprint the late DII_3 andalusite assemblages. DII_4 shear movement is therefore accompanied by a slight rise in pressure. DII_4 shear zones gradually increase in grade eastward along the Reynolds Range. This trend coincides with the variation in peak metamorphic grade attained during *M*II, indicating that the rocks had not yet fully cooled when DII_4 thrusting commenced.

*D*III–*M*III is late Devonian to Carboniferous in age and caused minor differential movement (<100 m) and retrogression along DII_4 shear zones.

INTRODUCTION

THE Reynolds Range in the central Arunta Block (Fig. 1) was multiply deformed and metamorphosed up to granulite-facies conditions around 1800 Ma ago (e.g. Warren & Stewart 1988, Clarke *et al.* 1989). The style of deformation and metamorphism in this terrain is similar to many other Proterozoic orogenic belts in that they typically display an anticlockwise pressure–temperature–time (*P–T–t*) path with high-temperature–low-pressure (HT–LP) metamorphism preceding deformation and relatively little post-orogenic uplift. Such orogenic belts are thought to be associated with crustal extension during continental break-up (Wernicke & Burchfield 1982, Sandiford & Powell 1986) and have been described in many Precambrian terrains. Australian examples include the Olary Block, South Australia (Clarke *et al.* 1987), the Mt Isa Inlier, Queensland (Pearson 1988), and the Arunta Block in central Australia (Warren & Stewart 1988). These Proterozoic orogenic belts are in marked contrast to Phanerozoic orogenic belts that are characterized by a clockwise *P–T–t* path, crustal thickening processes followed by regional Barrovian type metamorphism and uplift in response to erosion and extension (England & Richardson 1977, England & Thompson 1984).

Portions of the Arunta Block are recognized as HT–LP granulite terrains (Stewart *et al.* 1980, Warren & Stewart 1988) though little is known in detail about the structural constraints with respect to the metamorphism. The Reynolds Range is significant in that it has a well developed stratigraphy that enables an analysis of the major structures. Both stratigraphy and structures pass coherently through rapidly changing metamorphic terrains making it possible to reconstruct the evolving structures in HT–LP granulite conditions. In this paper we present an outline of the structural evolution and the related metamorphic events that can be observed in the Reynolds Range. We will demonstrate that the structural and metamorphic Proterozoic events (*D*I–*M*I and *D*II–*M*II) affect the Reynolds Range and the nearby Anmatjira Range in a very similar fashion. It is argued that these cycles are the regional expressions of orogenic events that affect the entire Arunta Block.

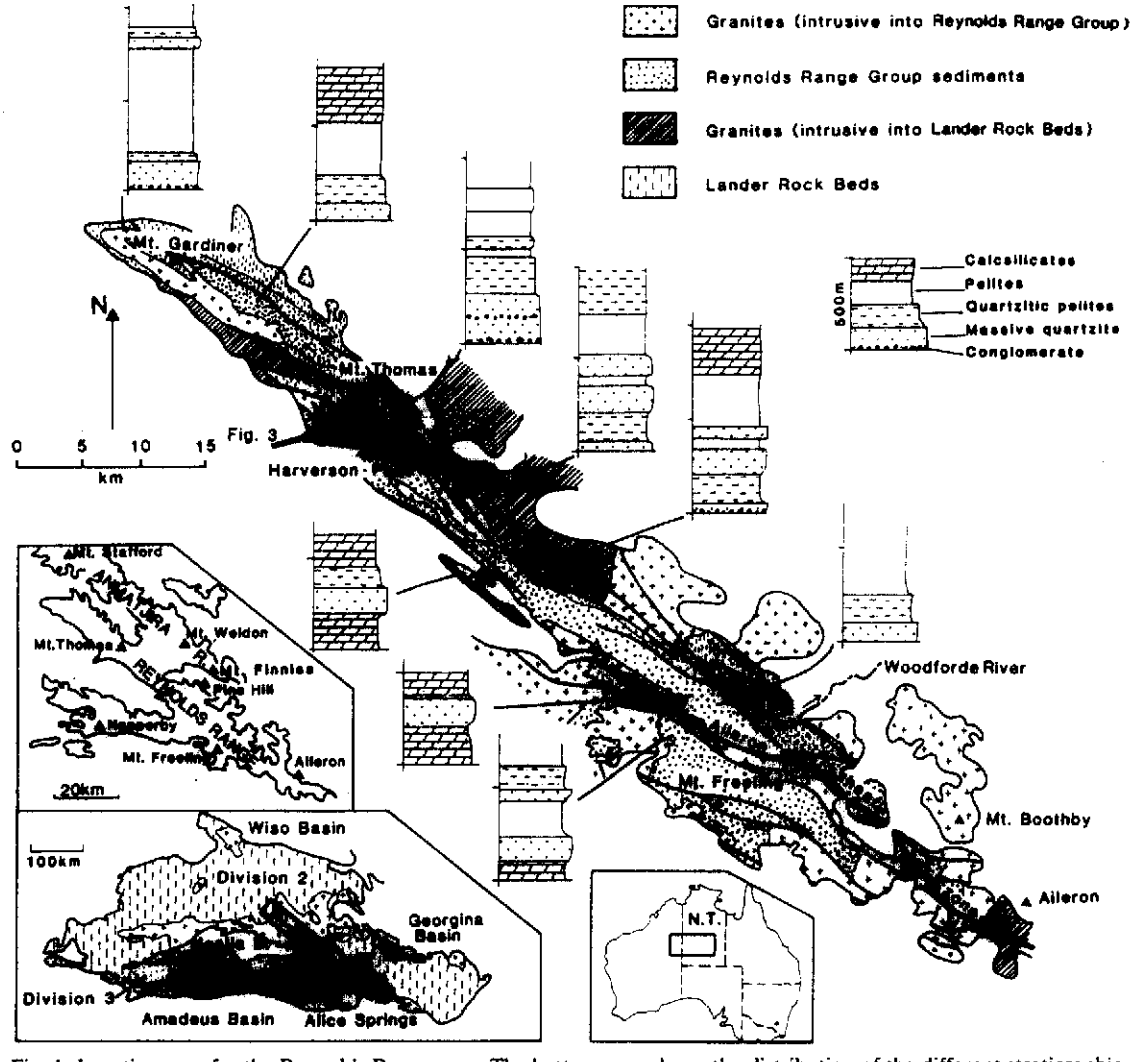

Fig. 1. Location map for the Reynolds Range area. The bottom map shows the distribution of the different stratigraphic units in the Arunta Block (after Shaw *et al.* 1984b). The main map shows the distribution of the stratigraphical units recognized in the Reynolds Range and includes a stratigraphic correlation for the sediments of the Reynolds Range Group.

REGIONAL GEOLOGY

The mid-Proterozoic deformation in the Reynolds Range pre-dated the development of a series of late Proterozoic sedimentary basins (Amadeus, Ngalia, Wiso, Georgina; Lindsay *et al.* 1987) around 900 Ma (Black *et al.* 1980). Stewart *et al.* (1980) and Stewart (1981) briefly discussed the Proterozoic deformation history and recognized three folding phases and two episodes of faulting. Four basic stratigraphic units can be distinguished in the Reynolds Range, based on basement–cover and granite–intrusive relationships (Fig. 1). The basement is represented by a folded immature sandstone and siltstone sequence, the Lander Rock Beds, which is intruded by granites (western part of the Mt Airy Orthogneiss, Mt Stafford Granite, Harverson Granite and Yakalibadgi Microgranite; Stewart 1981). An angular unconformity in the NW Reynolds Range separates the Lander Rock Beds from the mature shallow marine sediments of the Reynolds Range group that are characterized by a massive basal quartzite unit overlain by interlayered pelite, quartzite and calcsilicate. These units contain well preserved sedimentary structures such as ripple marks, cross-beds and slumps (Fig. 2a). Granites (e.g. Napperby Gneiss and Mt Boothby orthogneiss) intruding these sediments make up the fourth stratigraphic unit (Fig. 1). Individual units such as the basal quartzite are mappable for tens of km; from a greenschist-facies terrain in the NW Reynolds Range into a granulite-facies terrain to the north and east of the Woodforde River (Fig. 1). To the south of the Woodforde River a major shear zone separates the granulites from amphibolite-facies rocks (Stewart *et al.* 1980, Warren & Stewart 1988). The transition from greenschist-facies rocks to granulite-facies rocks in the central Reynolds Range is not a tectonic boundary. Stratigraphic units and structural trends pass coherently through this zone which is only 2 km wide and characterized by pervasive retrogression (Stewart *et al.* 1980).

DEFORMATION HISTORY

Three distinct structural–metamorphic cycles are involved in the evolution of the Reynolds Range. The deformations have been designated *D*I, *D*II and *D*III,

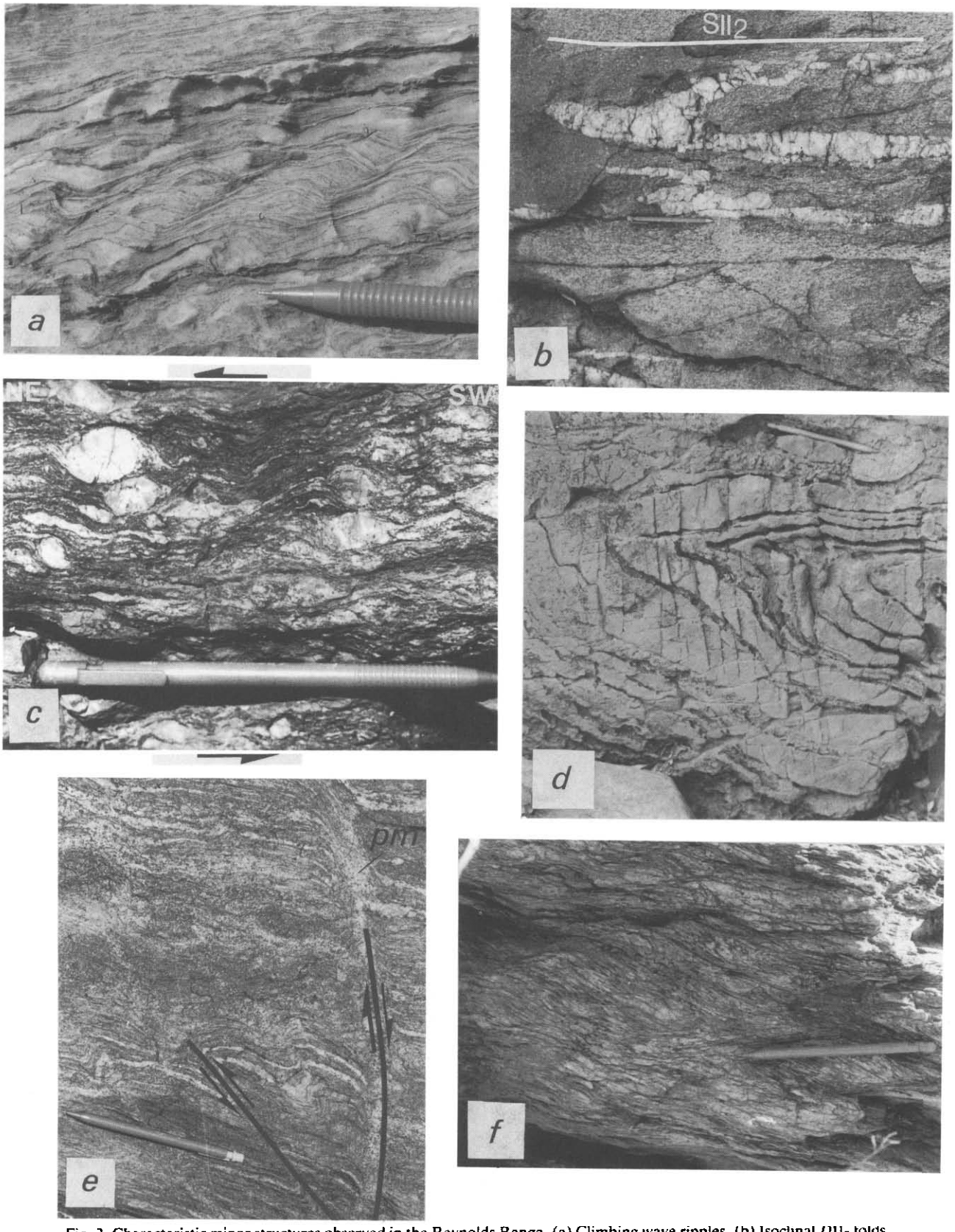

Fig. 2. Characteristic minor structures observed in the Reynolds Range. (a) Climbing wave ripples. (b) Isochinal DII_2 folds of quartz veins in granite that intruded during MI. (c) Mylonitic DII_2 fabric recording SW-over-NE sense of shear. (d) DII_2 fold overprinted by sub-vertical DII_3 cleavage. (e) Conjugate sets of DII_3 shear crenulations. Partial melt (pm) is concentrated along the shears. (f) $DIII$ mylonite fabric overprinted by shear bands.

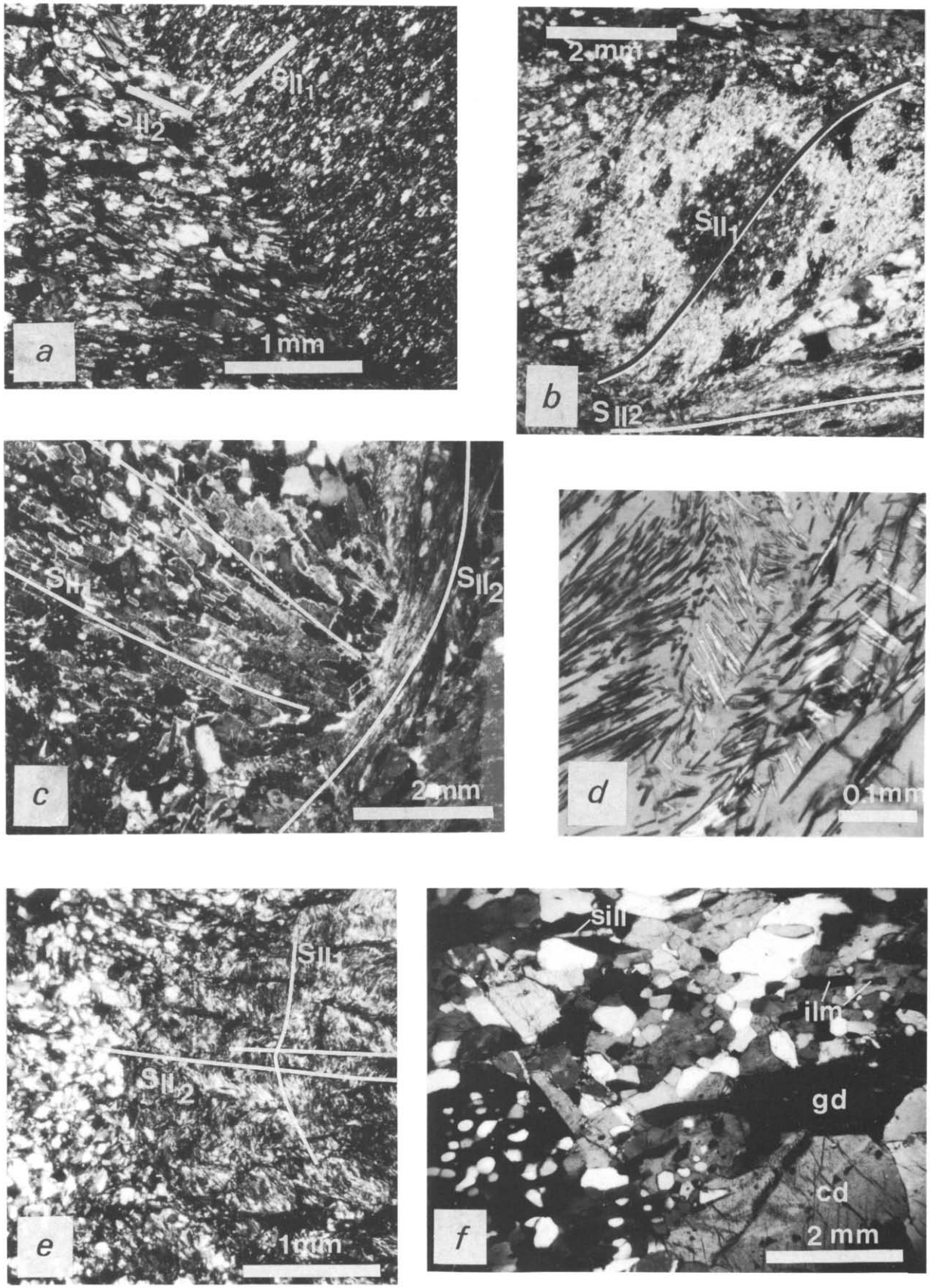

Fig. 4. Characteristic fabric elements (crossed polarized light). (a) Straight inclusion trails of quartz in andalusite define an internal fabric, SII_1, that makes an angle with the external fabric, SII_2. (b) Bent inclusion trail, SII_1, defined by quartz in andalusite which is wrapped in SII_2 crenulation cleavage. (c) Bent inclusion trail, SII_1, defined by biotite K-feldspar which is wrapped in SII_2 sillimanite fabric. (d) Crenulated SII_1 sillimanite in cordierite. (e) SII_2 crenulation cleavage. (f) High-grade SII_2 fabric defined by quartz sillimanite (sill), gedrite (gd), ilmenite (ilm) and cordierite (cd).

Table 1. Summary of the structural elements that compose the three deformational cycles

		Folding	Faulting	Cleavage
*D*I	1	N–S-trending, upright chevron folds	?	SI_1—axial planar slaty cleavage
*D*II	1	?	?	SII_1—sillimanite, mica fabric
	2	NW–SE-trending, tight, upright folds	Locally sheared out fold limbs	SII_2—penetrative sillimanite, mica, cordierite fabric
	3	Conjugate crenulation zones	—	SII_3—fracture solution cleavage
	4	Drag folding	NW–SE-trending, NE-dipping thrusts interconnected by an anastomosing pattern of steep shear zones	—
*D*III	1	Minor drag folding	NW–SE-trending anastomosing pattern of steep shear zones	—

and are accompanied by metamorphic events *M*I, *M*II and *M*III. The individual deformation events that constitute each cycle will be called DI_1, DI_2, etc. (see Table 1). In the adjacent Anmatjira Range (Fig. 1), different tectonic cycles were designated D_1–M_1, D_2–M_2, etc., and individual event D_{1a}, D_{1b}, etc. (Clarke *et al.* 1990, Collins *et al.* in press). A clear parallel exists between D_1–M_1 in the Anmatjira Range and *D*I–*M*I in the Reynolds Range. D_2–M_2, D_3–M_3 and D_4–M_4 recognized by Collins *et al.* (in press) and Clarke *et al.* (1990) in the Anmatjira and Reynolds Range are considered here to be part of the *D*II–*M*II tectonic cycle. The generally accepted convention in structural geology is to use D_1, D_2, etc., as individual structural events that occur within a tectonic framework (Hobbs *et al.* 1976). In this paper, *D*I, *D*II, etc., will be used to distinguish tectonic cycles and DII_1, DII_2, etc., to describe the distinct structural events that constitute each cycle.

Deformation D*I*

*D*I is related to the basement structures visible in the Lander Rock Beds in the NW Reynolds Range (Fig. 1). Folds in interlayered sandstone and shale have a tight to closed chevron type geometry, with wavelengths of 200–300 m. Within the fold hinges, an axial-planar fracture-solution cleavage is enhanced by the alignment of muscovite (SI_1). SI_1 is near vertical, trends NW–SE and makes an angle between 30° and 40° with the overlying sediments of the Reynolds Range Group. Removing the effects of later deformation (discussed below), SI_1 trended close to N–S and dipped moderately to the east. *D*I structures and fabrics become more intense to the north. This coincides with a rapid increase in the metamorphic grade from greenschist-facies to extreme low-pressure granulite-facies around Mt Stafford (*M*I, Vernon *et al.* 1989). SI_1 probably correlates with the upright S_{1c} fabric described in the Mt Stafford area by Collins *et al.* (in press) (Fig. 1).

In the low-grade north-west part of the Reynolds Range, the Reynolds Range Group sediments are separated from the Lander Rock Beds by an angular unconformity which is best displayed north of Mt Gardiner (Fig. 1). To the south-east of Harverson Pass (Fig. 1), the angular unconformity becomes indistinguishable from a normal stratigraphic contact even though the intensity of *D*II deformation is similar to that around Mt Gardiner (Fig. 1). It is likely that the unconformity did not exist in the SE Reynolds Range. This implies that the *D*I deformation events were localized in the Mt Stafford area.

Deformation D*II*

*D*II is related to penetrative deformation of the entire Reynolds Range. A metamorphic event (*M*II) attained peak conditions early during *D*II with highest grades reached in the Aileron–Mt Boothby area (Warren & Stewart 1988). During this cycle the relative timing of the different structural and metamorphic events remained identical along the entire length of the range with a transition from greenschist-facies (around 4 kbar and 450–550°C) in the north-west to granulite-facies in the south-east Aileron–Woodforde River area (4.5 ± 1 kbar and 700–800°C, Clarke & Powell personal communication, Warren & Stewart 1988). Granites that outcrop in the north-west part of the range were emplaced immediately predating *M*II (Fig. 3). Associated with these intrusives are 2–200 m wide contact metamorphic aureoles characterized by the growth of large (≤35 mm) andalusite porphyroblasts that contain aligned straight to slightly curved quartz inclusion trails reflecting an early fabric: SII_1 (Figs. 4a & b) which is interpreted as a prograde fabric evolving into the regionally dominant SII_2 fabric. In the higher grade terrains peak metamorphic mesoperthitic potassium feldspar and cordierite define SII_2 and contain straight to crenulated inclusion trails of sillimanite, biotite and quartz which define SII_1 (Figs. 4c & d). Evidence of this fabric on outcrop scale is uncommon. In places a strong layer parallel SII_1 cleavage is preserved and defined by white micas (in the north-west) or an alignment of sillimanite (in the south-east) along the hinges of FII_2 isoclinal folds (Fig. 4e).

The DII_2 event involved the formation and tightening of upright NW–SE-trending isoclinal folds that control the distribution of the stratigraphic units (Figs. 3 and 5). The larger scale FII_2 folds have wavelengths between 1 and 5 km. A penetrative subvertical NW–SE-trending fabric, SII_2, developed axial planar to these folds (Figs 2b & d). In the NW Reynolds Range SII_2 is a slaty cleavage defined by an alignment of muscovite, chlorite or biotite. In the south-east SII_2 is defined by a leucocratic layering and the preferred orientation of sillimanite, cordierite, orthopyroxene, ilmenite and biotite

(Fig. 4f). This assemblage defines the peak metamorphic assemblage in the SE Reynolds Range and therefore DII_2 occurred while MII peak metamorphic conditions prevailed. Sillimanite and micas also define a prominent mineral stretching lineation, LII_{2X} that plunges steeply towards the south-east (Fig. 5). The FII_2 folds and SII_2 fabrics can be followed continuously across the granulite–greenschist transition zone and fold geometries are identical irrespective of the metamorphic grade. FII_2 fold axes exhibit marked plunge changes on scales varying from a few cm up to several km and many of the macroscopic folds have an almost sheath-like geometry. From the north-west to the south-east of the Reynolds Range the folds become gradually tighter.

During progressive DII_2 flattening, SII_2 wrapped around porphyroblasts and conjugate sets of extensional shear bands and symmetrical cleavage boudins developed (Platt & Vissers 1980). The general symmetry of the DII_2 microstructures suggests that FII_2 folds were formed during progressive coaxial deformation. Locally SII_2 and LII_{2X} intensify and delineate distinct high strain zones (Fig. 5) that are situated in the limbs of tight folds. S–C fabrics and rotated blasts indicate that the deformation history in these zones was non-coaxial (Fig. 2c). These zones record both SW-over-NE and NE-over-SW movement and the continuity of the stratigraphy across the zones suggests that offsets are small (<1000 m). They are associated with the progressive tightening of the symmetrical FII_2 folds.

An evaluation of the DII_2 finite strain was undertaken using: (1) a point distribution analysis,the Fry analysis (Fry 1979), on large feldspar augen in deformed granites; (2) the R_f/ϕ technique (Ramsay 1967); or (3) by calculating the harmonic mean (Lisle 1985) of at least 20 quartzitic pebbles in metaconglomerates. The use of the Fry analysis was limited as augen gneisses that were clearly affected by DII_2 recorded no strain. This is explained as being the result of an original Poisson random distribution of the feldspar augen (Ramsay & Huber 1983). The results obtained from the pebbles exhibit a direct relationship between the pebble shape and the DII_2 fabric. The long axes of the pebbles (X) were aligned with LII_{2X} whereas the minimum axes lay normal to SII_2. Recorded strains are close to plane

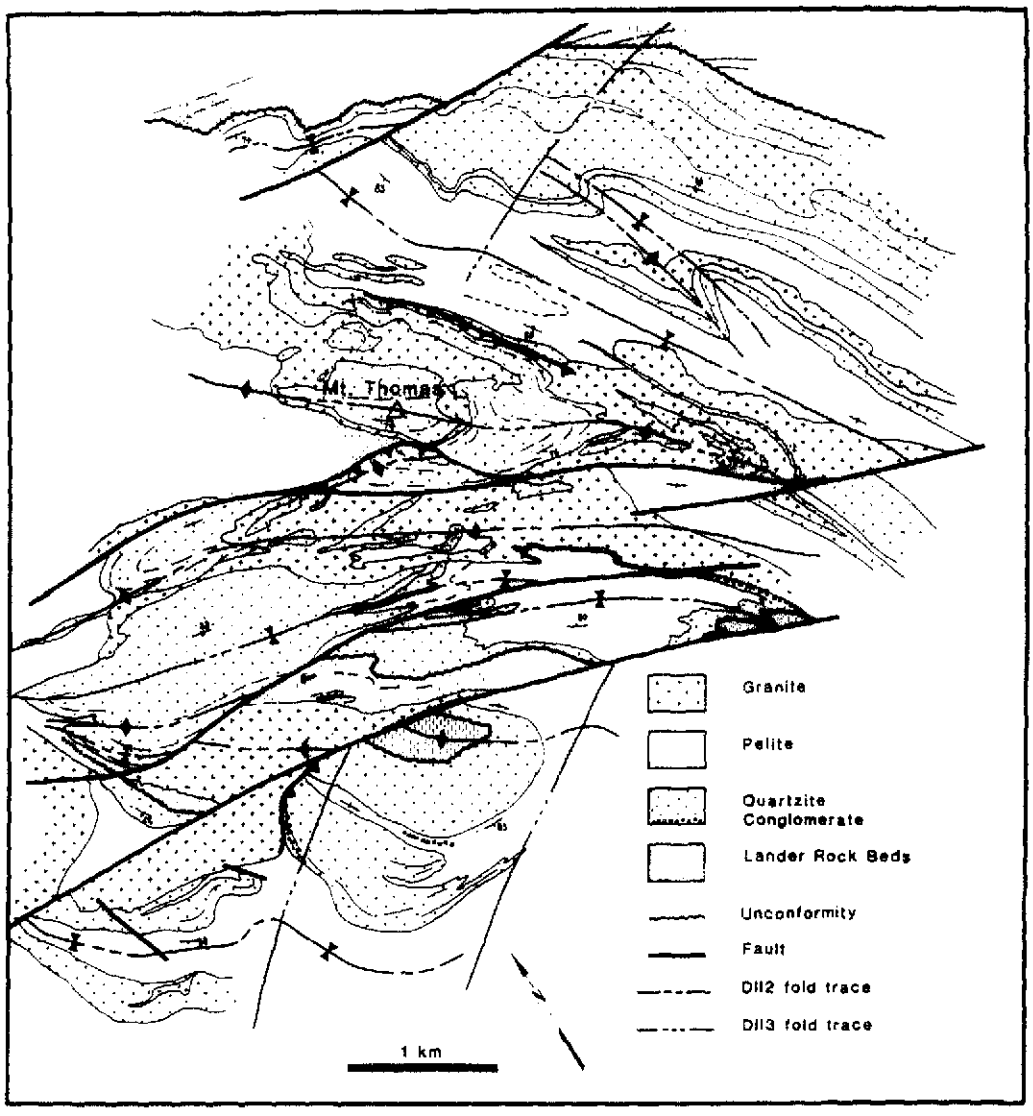

Fig. 3. Geological map of the Mt Thomas area, NW Reynolds Range.

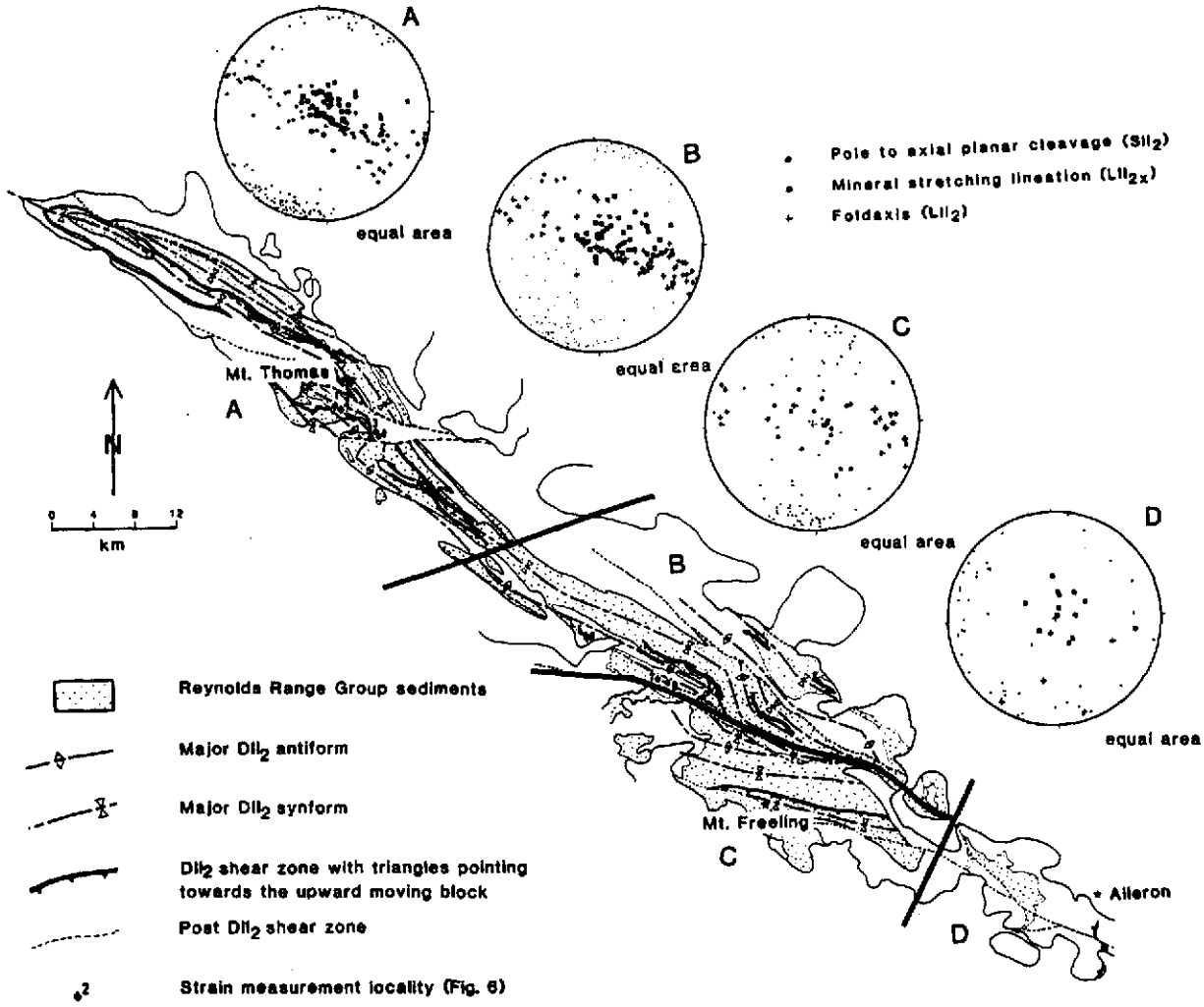

Fig. 5. Schematic structural map of the Reynolds Range showing the distribution of major DII_2 structures. The stereonets (equal-area, lower-hemisphere projection) show the orientation of the related fabric elements. Sub-area A represents the greenschist-facies terrain dominated by DII_2 structures. The effects of DII_3 are minor and localized. Sub-area B is characterized by partly retrogressed amphibolite- and granulite-facies terrains dominated by DII_2 structures. Sub-area C is characterized by partly retrogressed amphibolite- and granulite-facies terrains. DII_2 structures are prominent and extensively reworked during DII_3. Sub-area D is characterized by granulite-facies terrains. Macroscopic DII_2 structures are almost impossible to recognize due to migmatization and DII_3 reworking.

strain with a tendency to apparent constriction (Fig. 6). The magnitude of stretching achieved during this deformation is between 150 and 300% with the highest values involving the non-coaxial high strain zones.

Migmatization during DII_2 is evident in the granulite terrain and is particularly widespread in the pelites belonging to the Reynolds Range Group and the granitic gneisses (Napperby Gneiss, Mt Airy Orthogneiss). Within the pelitic gneisses, SII_2 is partly defined by a leucocratic layering that is interpreted as a melt segregation. There is little evidence for large-scale mobilization of melt although minor melt pockets, containing cordierite/quartz or garnet/quartz symplectites, occur preferentially along DII_2 boudin necks (Fig. 7).

DII_3 structures are associated with near vertical asymmetrical shear bands and conjugate sets of crenulation bands which geometrically resemble conjugate kink bands. The scale of the crenulation bands varies from a width of a few cm to widths of 5 km (Figs. 2e and 8). Within the larger scale crenulation bands, large sections of earlier folds and fabrics are rotated to a near recumbent position (Fig. 8). The dominant set of crenulation bands is upright and trends ENE–WSW crossing the general strike of the Reynolds Range. Crenulations generally plunge moderately (0–70°) to the east and verge towards the SSE and are associated with an oblique NE-over-SW displacement across the zones (Fig. 8). The conjugate to this set trends NW–SE along the main trend of the range with deformation localized in narrow 0.02–150 m wide upright zones that nearly parallel SII_2. Crenulations that belong to the latter set are developed together with the dominant ENE–WSW set in more homogeneous rock types such as the Napperby Gneiss. They may plunge between 30° to SE and 75° to NW but are generally steep and verge to SW, in accordance with oblique NE-over-SW displacements across the associated zones. The largest scale crenulation bands associated with the minor set have a width of several 100 m and occur in the Mt Freeling area (Fig. 1). Disharmonic box-type interference folds occur where both sets of crenulations intersect. Except along more intensely crenulated zones, no penetrative fabric formed

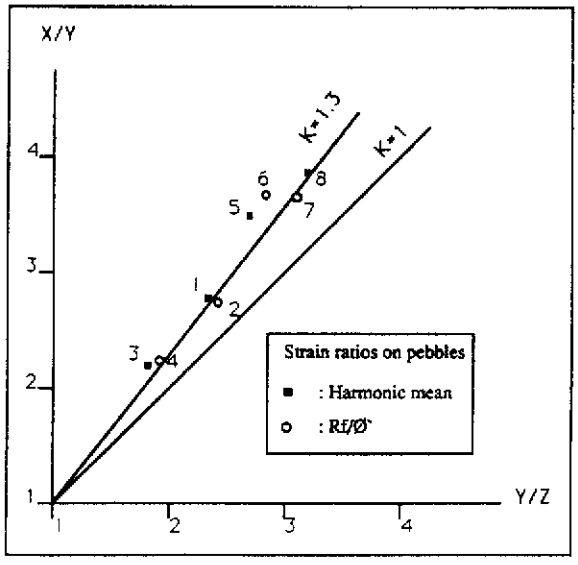

Fig. 6. Flynn diagram displaying the finite strain determined from the axial ratios of quartzite pebbles in metaconglomerates. The different numbers indicate the locations where the measurements were taken, as indicated in Fig. 5.

during DII_3. Locally a fracture cleavage (SII_3) developed in the granitic gneisses and a weak retrograde sillimanite–biotite fabric formed in some pelitic gneisses (Fig. 2d). The intensity of DII_3 defomation increases towards the south-east and is greatest south-east of the Woodforde River.

In the NW Reynolds Range DII_2 and DII_3 can be recognized as two distinct deformation events separated by an episode of retrogression. During DII progressive deformation SII_2 was compressed symmetrically around MII andalusites. The andalusite subsequently retrogressed to clots of colourless mica which were crenulated during DII_3. Towards the south-east the transition from DII_2 to DII_3 is gradational and covers a series of overprinting conjugate sets of asymmetrical crenulation bands, asymmetrical boudins and extensional shears. Retrogression commenced prior to and continued during DII_3. This can be illustrated by the evolutional history of the partial melts generated during MII. Within the pelitic granulites (composed of 5–30% quartz, 5–30% cordierite, 0–40% sillimanite, 0–15% biotite, 5–40% K-feldspar and less than 5% plagioclase, garnet, spinel, ilmenite and orthopyroxene) the melts had largely solidified before the onset of DII_3 crenulation. In the extensively migmatized granitic basement rocks (especially the Napperby Gneiss) partial crystallization of melt took place after DII_2 but up to 30% melt, with a minimum melt composition, was still present during DII_3. The melt occurs preferentially along dilatational sites such as the conjugate set of crenulation bands (Fig. 2e). Migration of the melt took place along these zones towards the boundary with the overlying sediments where the melt collected into layer-parallel pockets with lateral distributions of several hundred metres and widths of ≤25 m. Occasionally these pockets pierced the boundary and intruded the sediments. After the crystallization of the melt, coarse pegmatites composed of quartz, K-feldspar and plagioclase with up to 10 cm booklets of biotite and muscovite and occasionally coarse tourmaline and epidote intruded the metasediments. The pegmatites are intruded by quartz–tourmaline veins. Retrogressive assemblages that are observed as haloes around the intruded melts and pegmatites include quartz, epidote, tremolite, muscovite, biotite, chlorite and albite in the calc silicates and andalusite, green biotite, chlorite, rutile and muscovite in the pelitic gneisses. Retrograde andalusite is restricted to the area south-west of Mt Boothby. These assemblages do not define any deformational fabrics and are the result of an influx of retrogressive fluids released

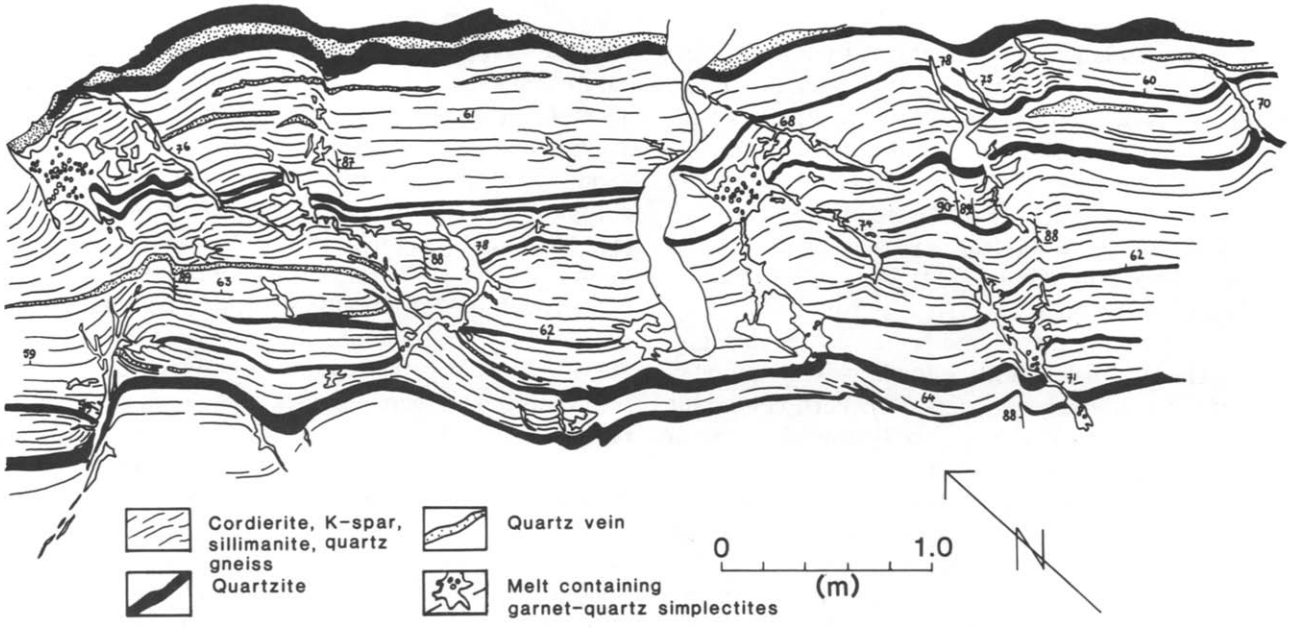

Fig. 7. Sillimanite, cordierite, potassium feldspar, quartz, biotite gneiss, alternating with quartzite, contains pockets of partial melt that have migrated towards dilatational sites such as boudin necks. The melt pockets contain garnet–quartz simplectites in a matrix of predominantly quartz and potassium feldspar.

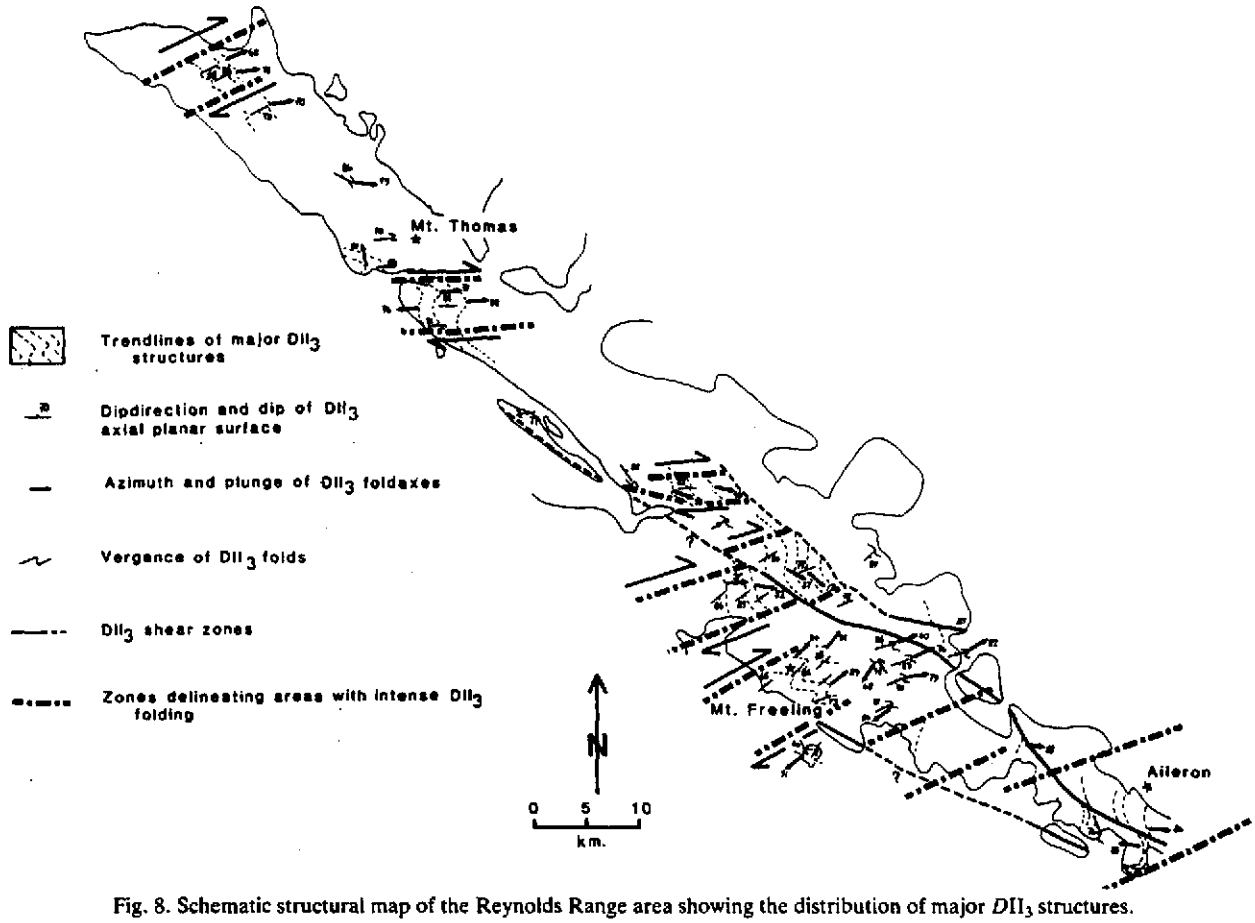

Fig. 8. Schematic structural map of the Reynolds Range area showing the distribution of major DII_3 structures.

during melt crystallization. Almost complete retrogression of the granulite–greenschist transition zone occurred during DII_3.

DII_4 is associated with a system of major NE-dipping thrusts interconnected by numerous smaller shear zones (Fig. 9). DII_4 faulting is most intense in the SE Reynolds Range. Towards the north-west the number of DII_4 shear zones and their individual widths decreases and movement directions change from dip-slip NE-over-SW thrusting to dextral strike-slip. In the SE Reynolds Range a system of major, 80–200 m wide NW–SE-trending mylonite zones can be recognized (Fig. 9). These zones dip between 40° and 55° towards NE and record down-dip NE-over-SW movement. The major shears are interconnected by a complex system of 5–60 m wide steeply dipping shear zones with mylonitic lineations plunging towards the NE at moderate angles (Fig. 9). The sense of movement on the minor shears is usually in accordance with the main NE-over-SW movement. Each separate fault block is truncated by numerous 0.5–15 cm wide mylonite and ultra-mylonite zones. Locally, cm-scale DII_4 ultramylonite zones preferentially occur along DII_3 shear bands and crenulation zones, from which they seem to have evolved.

DII_4 shear zones are the loci for extensive retrogression. The shears are surrounded by a retrogressive halo which has a width that is generally 2–3 times the width of the associated mylonite zone. Quartz veining and mylonite folding are common. The grade of the shear zones varies along with the length of the range. In the NW Reynolds Range the mylonitic fabric, SII_4 and LII_{4X} is defined by quartz, chlorite and muscovite. Towards the south-east biotite occurs instead of chlorite. Along the Aileron shear at the Woodforde River north of Mt Freeling (Fig. 1) poorly oriented kyanite and staurolite and garnet have overgrown a mylonitic biotite–quartz fabric. Further south-east along this shear zone the fabric is defined by oriented kyanite, staurolite, quartz, biotite and rutile. North-east towards Mt Boothby lineated sillimanite is overgrown by both lineated and randomly oriented kyanite. North of Mt Boothby the sillimanite fabric is overgrown by oriented staurolite and poorly oriented kyanite, garnet and staurolite. The grade of the shear zones increases towards the east where they reach amphibolite grade (5–6 kbar, 500–600°C). This increase in grade of the shear zones coincides closely with the variation in peak metamorphic grade attained during MII. This means that the rocks were not yet fully cooled when DII_4 thrusting commenced and illustrates the close relationship between DII_4 and the preceding granulite-facies event.

During DII essentially penetrative coaxial deformation (DII_2) evolved into localized non-coaxial deformation (DII_3–DII_4). The main shortening direction (NE–SW) remained constant.

Deformation DIII

$DIII$ is characterized by non-coaxial deformation on narrow high strain zones. During $DIII$ nearly all DII_4 shear zones are reactivated either passively, as fluid conduits causing retrogression of DII_4 fabrics, or active-

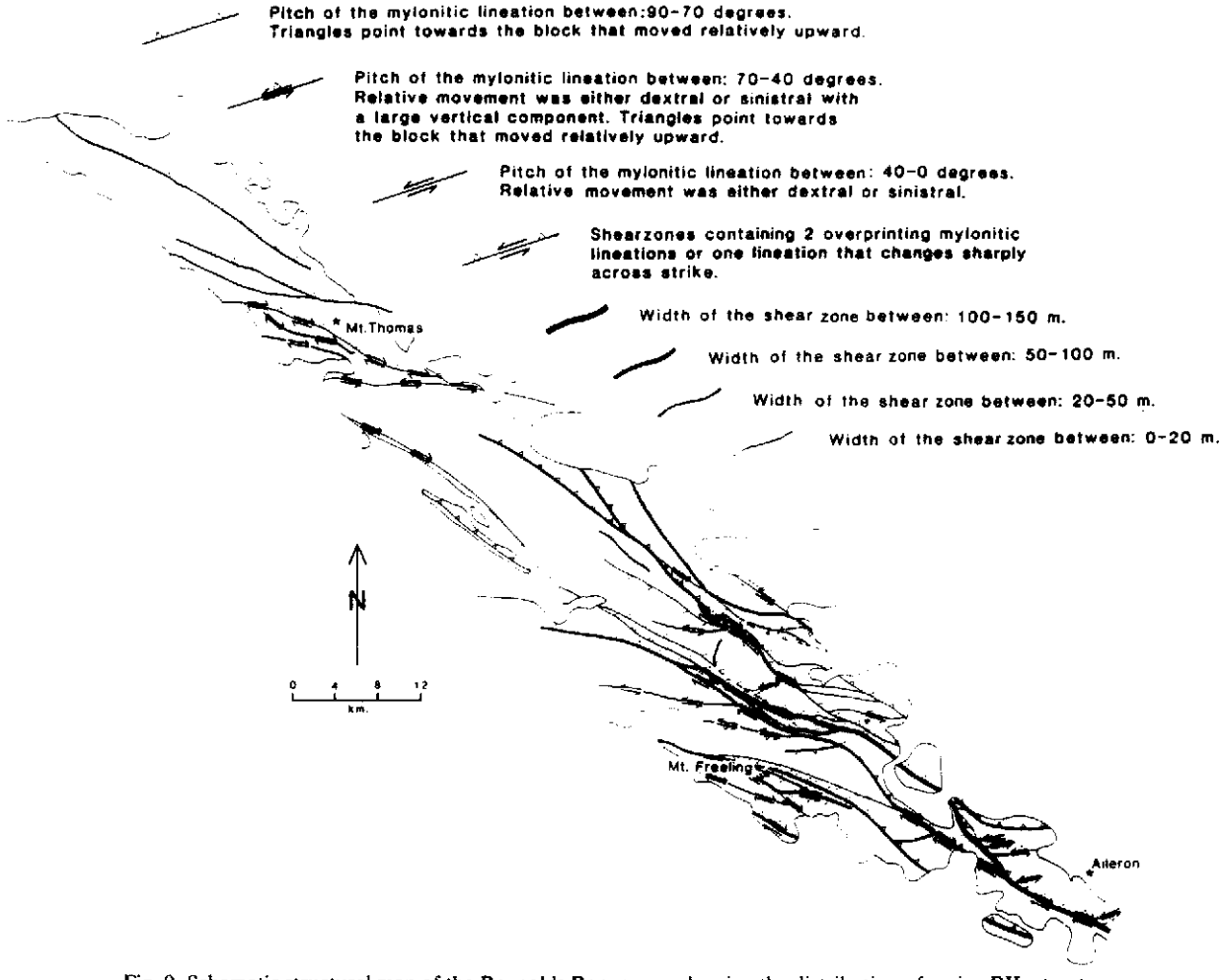

Fig. 9. Schematic structural map of the Reynolds Range area showing the distribution of major DII_4 structures.

ly as shear zones likewise associated with retrogression. *D*III shear zones are up to 20 m wide and generally occur as narrow anastomosing zones within DII_4 shears. They are characterized by their micaceous retrogressive nature, the development of distinct shear bands (Fig. 2f) and small displacements (<100 m). Overprinting muscovite–chlorite lineations indicate that the *D*III shear zones record two distinct phases of ductile shear. An earlier phase is related to N-over-S reverse movement and a later phase is related to dextral strike-slip.

*D*III was accompanied by a greenschist-facies metamorphic event (*M*III) along the high strain zones causing retrogression of the amphibolites and granulites to muscovite–chlorite–biotite schists. The final stages of movement along the retrogressive shear zones produced crenulations and kink zones.

AGE OF DEFORMATION CYCLES

U–Pb ion–microprobe data obtained from zircons extracted from gneisses in the Reynolds and Anmatjira Ranges present a framework of dates to which the previously described events can be fitted (Clarke *et al.* 1990, Collins *et al.* in press). Metamorphosed and deformed (*D*I–*M*I) Lander Rock Beds were intruded by megacrystic granites containing metamorphic zircons dated at 1820 Ma. Charnockites in the Mt Weldon area (central Anmatjira Range, Fig. 1) contain a main population of zircons that give an age of 1760 Ma and a second zircon population that is dated at 1585 Ma. Napperby Gneiss from the central Reynolds Range contains a complex population of zircons giving three distinct ages. Early zircon grains contain cores that are dated at 1760 Ma and rims with a mean age of 1730 Ma while a population of new grains give an age of 1650 Ma. The zircons were extracted from bulk samples that contained granulitic gneiss and a seemingly undeformed melt phase.

Clarke *et al.* (1990) and Collins *et al.* (in press) interpret the dates to reflect three distinct granulite events followed by several episodes of thermal remobilization at amphibolite grade. A M_1 granulite-facies event occurred around 1820 Ma in the Mt Stafford area. The early zircons from the charnockite in the Mt Weldon area are interpreted to represent a second granulite-facies event, M_2, at 1760 Ma. The 1760 Ma obtained from the Napperby Gneiss is interpreted as an emplacement age and is linked to M_2. The gneiss underwent a third granulite-facies event, M_3 at 1730 Ma, that affected

the SE Reynolds Range. The 1650 Ma age in the Napperby Gneiss and the 1585 Ma in the charnockites are interpreted as amphibolite-facies events associated with remobilization and crystallization of melt. The currently visible effects of deformation associated with M_1, M_2 and M_3 are interpreted to be almost entirely restricted to the Mt Stafford area, the SE Anmatjira Range and the SE Reynolds Range, respectively. Recumbent fabrics ($S_{1a,b}$, S_2, S_3, Collins *et al.* in press) are interpreted to have formed during each of these granulite events. The only deformational event that has affected both ranges (D_4) consists of relatively late upright folds that deform a partial melt vein which is interpreted to have formed at 1585 Ma.

Based on detailed structural mapping along the entire Reynolds Range, we propose a reinterpretation of the above dates. In accordance with Clarke *et al.* (1990) and Collins *et al.* (in press) the 1820 Ma ages are correlated with the *D*I–*M*I events centred in the Mt Stafford area. At the Napperby Gneiss sample locality a series of *D*II events can be recognized. The main gneissic fabric, $S\text{II}_2$, is crenulated along $D\text{II}_3$ crenulation zones. Garnet bearing partial melt occurs preferentially along the axial planes of the $D\text{II}_3$ crenulations and the gneiss and the melt phase are cross-cut by a $D\text{II}_4$ shear zone that contains ultramylonites. Retrogression associated with the shear zone affects the entire outcrop. Further muscovite retrogression has taken place along these zones during *D*III. Thin section work reveals that the main gneissic fabric, $S\text{II}_2$, is defined by a coarse dark brown biotite. Large irregular zircons as well as cored euhedral zircons oriented within $S\text{II}_2$ are common. Dynamic recrystallization of quartz and K-feldspar and retrogression of the brown biotite to a green biotite, rutile and muscovite is probably related to the nearby shear zone. The partial melt is made up of quartz, K-feldspar and garnets with remnants of brown biotite. Zircons are rare, generally small and both rounded and euhedral. The melt phase was clearly corrosive to zircons which went into solution. Some euhedral clear zircon has grown with retrograde biotite along cracks in the garnet. The shear zone consists of dynamically recrystallized quartz and K-feldspar, and green–brown biotite is present in large amounts and occurs along distinct shear bands. The shear zone is rich in zoned clear euhedral zircons of various sizes that are aligned within the mylonitic foliation. 1760 Ma is taken as the date at which zircon growth started and might coincide with the emplacement date of the precursor granite though alternatively it might date the onset of $M\text{II}_2$ metamorphism. Metamorphic zircon growth continued till about 1730 Ma; till melts that were corrosive to zircons become a dominant feature in the gneiss preventing further zircon growth. This happens while peak metamorphic conditions are reached during $D\text{II}_2$. Therefore the interpretation of the 1650 Ma age as a separate thermal phase during which zircons grew in a melt (Clarke *et al.* 1990, Collins *et al.* in press) is unlikely. We believe that the new zircon population with an age of 1650 Ma has grown in a fluid phase during $D\text{II}_4$ thrusting event. It is emphasized that $D\text{II}_2$, $D\text{II}_3$ and $D\text{II}_4$ represent continuous, evolving deformational events under waning metamorphic conditions that are temporally and spatially related. Direct field observations, discussed in the next section, favour an interpretation combining the Mt Weldon and Reynolds Range events (M_2 and M_3 in Clarke *et al.* 1990, Collins *et al.* in press) in one *D*II–*M*II tectonic event. In summary, *D*II commenced with the emplacement of granites and the build-up of heat around 1760 Ma. Peak metamorphic conditions were reached at 1730 Ma contemporaneous with upright folding. Subsequent cooling and non-coaxial deformation on shear zones took place until 1650 Ma. Amphibolite-grade conditions prevailed post $D\text{II}_4$, as recognized in the SE Reynolds Range and the Anmatjira Range from unoriented kyanite, staurolite, biotite assemblages overprinting the $D\text{II}_4$ mylonitic fabrics. The rare 1585 Ma old zircons from the Mt Weldon area that are interpreted to have grown in partial melt (Collins *et al.* in press) have possibly grown in response to a further fluid flux on the $D\text{II}_4$ shear zones while high-grade post-tectonic conditions prevailed.

The Lander Rock Beds were deposited prior to 1820 Ma as they are intruded by 1820 Ma old granites. They may be equivalent to the marine sediments and 1880–1870 Ma old felsic volcanics of the Warramunga Group in the Davenport Province north of the Reynolds Range (Shaw & Stewart 1975, Black 1984). The Reynolds Range Group sediments are intruded by the Napperby Gneiss and unconformably overlie the 1820 Ma granites. Therefore they were deposited between 1820 and 1760 Ma. These sediments possibly correlate with the fluviatile and shallow marine sediments and ±1810 Ma felsic volcanics that make up the Hatches Creek Group in the Davenport Province (Shaw and Stewart 1975, Black 1984). A summary of the different ages incorporating the structural–metamorphic cycles affecting the Reynolds Range is presented in Table 2.

Table 2. Summary of the structural–metamorphic evolution of the Reynolds Range with respect to zircon dates obtained by Collins *et al.* (in press).

	Age (Ma)	Geological event
	1870–1830 ?	Deposition of the Lander Rock Beds
cycle I	1820	*D*I, *M*I centred around Mt Stafford (affected the NW Reynolds Range) Intrusion of granites
	1820–1760	Deposition of the Reynolds Range Group
	1760	Intrusion of granites (e.g. Napperby Gneiss)
cycle II	1730	$D\text{II}_1$–$D\text{II}_2$ progressive deformation, *M*I $D\text{II}_3$, cooling of metamorphic peak and mobilization of granitic melt
	1650	$D\text{II}_4$, shear zone development and uplift
cycle III	380–320	$D\text{III}_1$, *M*III, shear zone development and uplift

DISCUSSION

The evolution of the Reynolds Range should be viewed in terms of three distinct structural–metamorphic cycles. The first Proterozoic structural–metamorphic cycle, *D*I, only affected the basement rocks in the north-west and was associated with a low-pressure granulite-facies metamorphic event, *M*I, around Mt Stafford in the NW Anmatjira Range (Vernon *et al.* 1989). *D*II commenced with the formation of a fabric, SII_1, preserved as inclusion trails in porphyroblasts. DII_1 represents the early stage of a progressive folding and flattening event that culminated during DII_2. The DII_2 deformation is associated with the formation of tight to isoclinal NW–SE-trending upright folds. Progressive flattening produced their sheath like geometry. DII_2 strain conditions were very homogeneous along the Range and approached plane strain. From a lack of asymmetrical kinematic indicators (Platt & Vissers 1980, Simpson & Schmidt 1983) it appears that the deformation history was dominantly coaxial. Non-coaxial deformation occurred along a number of narrow high strain zones in the limbs of FII_2 folds and record both NE- and SW-directed thrusting. Both basement rocks and overlying sediments are equally affected by DII_2. DII_3 structures are associated with conjugate sets of crenulation zones at scales that vary from several cm to 5 km. Crenulations display a SE vergence along ENE–WSW-trending zones and a SW vergence along NW–SE-trending zones with each individual zone recording non-coaxial strain histories. On the scale of the entire Reynolds Range the DII_3 zones form a conjugate pattern that is dominated by the ENE–WSW-trending set and the overall DII_3 strain history records large-scale NE-over-SW movement. With progressive deformation strain localization occurred within DII_4 shear zones that involved large-scale NE-over-SW thrusting on NE-dipping NW–SE-trending mylonite zones. Amphibolite-facies metamorphism accompanying DII_4 is limited to the areas that underwent *M*II granulite-facies metamorphism indicating the thermal anomaly associated with *M*II had not yet fully cooled at the onset of DII_4. During *D*III renewed thrusting and greenschist-facies retrogression occurred on most DII_4 zones. Offsets during this event were minor. It seems unlikely that movements on the *D*III shear zones exposed in the Reynolds Range are responsible for the uplift of the granulite terrains to present crustal levels (Collins & Teyssier 1989).

A paucity of detailed *D*I structural data makes it difficult to estimate the orientation of the early compressional direction, σ_1. During *D*II, σ_1 was continuously directed NE–SW while structures evolved from penetrative coaxial deformation during DII_2, via broadly localized non-coaxial deformation resulting from NE-over-SW displacement on a conjugate set of crenulation zones during DII_3, to distinctly localized non-coaxial deformation associated with NE-over-SW movement on shear zones during DII_4. This evolution of structural styles coincides with the cooling of the *M*II metamorphic event. During *D*III the sense of movement on *D*III shear zones indicates that σ_1 was also directed NE–SW.

*D*II deformation closely followed a low-pressure granulite-facies metamorphic event (*M*II, 1730 Ma) that was associated with a thermal anomaly. Highest grades are recorded in the SE Reynolds Range ($P = 4.5$–6 kbar, $T = 700$–800°C). Deformation proceeded while the thermal anomaly cooled (DII_3, DII_4). Oriented sillimanite + biotite assemblages that formed early during DII_3 and unoriented andalusite + chlorite + muscovite assemblages that formed late during DII_3 indicate that cooling of *M*II was initially isobaric. During DII_4 thrusting staurolite + garnet + biotite + quartz and biotite + staurolite + kyanite + quartz assemblages overprint the late DII_3 andalusite assemblages indicating a slight rise in pressure (500–600°C, ±5–6 kbar). The relative timing of *M*II and the *D*II deformation events is identical along the entire range and the intensity of the separate events increases dramatically with increasing metamorphic grade. *D*III is Devonian to Carboniferous in age and is associated with regional greenschist-facies metamorphism.

Comparison of the Proterozoic structural events observed in the Reynolds Range and the nearby Anmatjira Range shows similarities in style and temporal relationships. The structural–metamorphic events recognized in the Mt Stafford area (Clarke *et al.* 1990, Collins *et al.* in press) correlate with the *M*I–*D*I events recognized in the Lander Rock Beds in the NW Reynolds Range. Restored *D*I structures show similar structural trends and geometries as F_{1c} folds recognized by Collins *et al.* (in press). Structures associated with the main granulite-facies metamorphic event recognized in the SE Anmatjira Range are similar to *M*II–*D*II events recognized in the Reynolds Range. Figure 10 shows two cross-sections; one across the Mt Weldon area in the central Anmatjira Range (Fig. 1) and one transecting the central Reynolds Range. In the Anmatjira Range tight upright NW–SE-trending folds are associated with a penetrative granulite-grade fabric (S_{2b}, Clarke *et al.* 1990) which formed directly after peak metamorphic conditions were reached (M_2, Clarke *et al.* 1990). These structures are refolded in large-scale conjugate crenulation zones (F_4, Clarke *et al.* 1990) that form broad SW-verging warps which rotated large sections of the Anmatjira Range to a near recumbent position as can be seen at Mt Weldon (Fig. 10). Another excellent example of this occurs at Mt Finniss (Fig. 1) which is situated at the intersection of a conjugate set of 1–2 km wide crenulation bands. Clarke *et al.* (1990) and Collins *et al.* (in press) interpreted the crenulation zones as D_4 upright folds that folded an earlier recumbent fabric (S_{2b}). The above structures are crossed by shear zones that contain sillimanite fabrics overgrown by poorly oriented staurolite. Many of these shear zones which Collins & Teyssier (1989) and Collins *et al.* (in press) attributed to the Alice Springs Orogeny, show later greenschist-facies retrogression. The composite history of the shear zones suggests that they had an early amphibolite-grade history (DII_4) overprinted by a

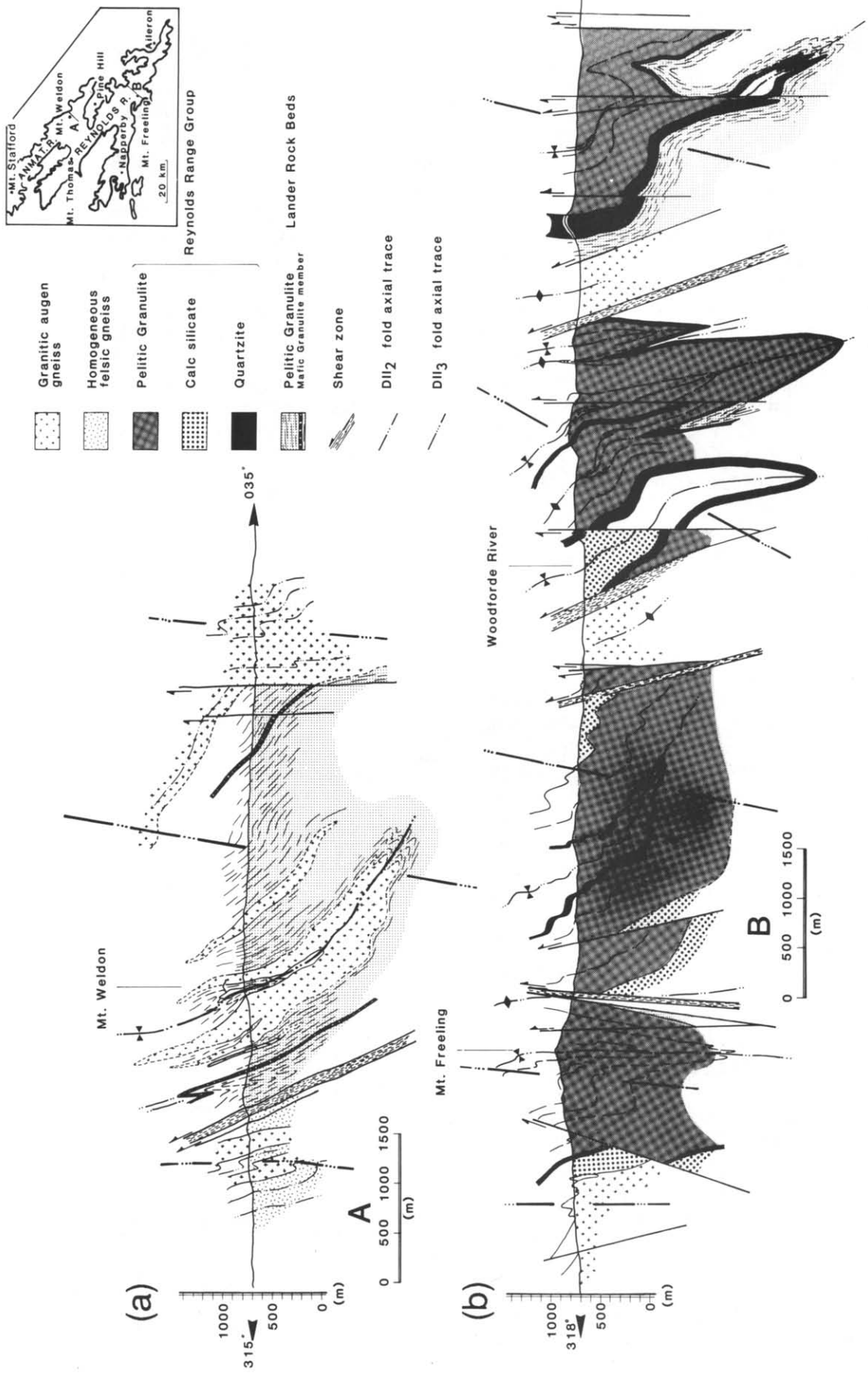

Fig. 10. (a) Structural cross-section A through Mt Weldon in the central Anmatjira Range and (b) Structural cross-section B through Mt Freeling in the central Reynolds Range.

greenschist-facies retrogression (DIII, Alice Springs Orogeny), Clarke *et al.* (1990) and Collins *et al.* (in press) argue that the penetrative deformation and metamorphism in the Reynolds and Anmatjira Ranges was caused by separate structural–metamorphic events (D_2–M_2 in the Anmatjira Range, D_3–M_3 in the Reynolds Range) and that the only deformation affecting both ranges was a later upright folding event (D_4). This structural–metamorphic framework is largely based on the zircon dating carried out by Collins *et al.* (in press) and is not in accord with the interpretation presented here. It is unlikely that penetrative high-grade compressional deformation accompanied by granulite-facies metamorphism occurred in restricted areas such as the SE Reynolds Range and the SE Anmatjira Range. We therefore propose that the Reynolds Range and the Anmatjira Range are affected by DII in a similar fashion. D_2–M_2, D_3–M_3 and D_4–M_4 of Collins *et al.* (in press) are part of the same DII–MII event that affected both ranges. Initially upright $D\text{II}_1$–$D\text{II}_2$ structures were rotated into a recumbent position along $D\text{II}_3$ crenulation bands (Fig. 10). Both areas were then cross-cut by similar complex shear zones ($D\text{II}_4$, DIII). Throughout the area, the regional change in grade of the $D\text{II}_4$ shear zones coincides with the variation in peak metamorphic grade. Clarke *et al.* (1990) calculated slightly higher peak metamorphic conditions in the Mt Weldon area than in the SE Reynolds Range. This is likely to reflect the effects of $D\text{II}_4$ thrusting.

Elsewhere in the Arunta Block a very similar tectonic history exists. In the Strangways Range and Harts Range 200–300 km SE of the Reynolds Range two high-grade granulite-facies events have been recognized (Warren 1983, Shaw & Langworthy 1984, Shaw *et al.* 1984a,b, Page 1988). A first event, the Strangways event, occurred around 1800 Ma and the second one, the Aileron event, occurred around 1700 Ma (Black *et al.* 1983). These terrains are cross-cut by shear zones that are very similar to the $D\text{II}_4$ shear zones described in this paper (e.g. the Yambah schist and Anuma schist, Shaw & Langworthy 1984, Shaw *et al.* 1984b). Therefore we suggest that the structural–metamorphic history recognized in the Reynolds Range is the local expression of a series of large-scale orogenic events that affected large sections of the Arunta Block.

CONCLUSIONS

(1) Three distinct structural–metamorphic cycles designated DI–MI, DII–MII and DIII–MIII affect the Reynolds Range.

(2) The DI–MI episode took place around 1820 Ma and only affected the NW Reynolds Range.

(3) DII–MII occurred between 1760 and 1650 Ma and caused pervasive deformation and metamorphism along the entire Reynolds Range. The DII tectonic cycle commenced with the intrusion of granites around 1760 Ma. Peak metamorphic conditions were reached around 1730 Ma while penetrative coaxial deformation associated with upright folding took place. During subsequent isobaric cooling deformation gradually became constricted to large-scale conjugate sets of shear bands along which large sections of previously upright structures are rotated to a recumbent position. Eventually distinct shear zones developed that were active until 1650 Ma and recorded NE-over-SW displacements. During DII the shortening direction remained NE–SW.

(4) DII structural events are coherent along the entire Reynolds Range irrespective of the metamorphic grade.

(5) The change in grade of the $D\text{II}_4$ shear zones coincides with the change in grade that existed during MII. Since MII is a high-temperature–low-pressure granulite event associated with a thermal anomaly, this means that the terrain had not fully cooled at the onset of $D\text{II}_4$ thrusting.

(6) DIII–MIII is late Devonian to Carboniferous in age and is associated with reactivation of $D\text{II}_4$ shear zones and retrogression to greenschist facies. Offsets on DIII shear zones are generally small.

(7) The tectonic cycles recognized in the Reynolds Range correlate with similar events in the adjacent Anmatjira Range.

Acknowledgements—Fieldwork for this project was supported by a grant from the Australian Research Council. We are also indebted to the Northern Territory Geological Survey for their support while undertaking fieldwork. We would like to thank Tony Norman, Martin Hand and Bill Collins for numerous stimulating discussions and Bill Collins and M. Rickard for revisions on an earlier version of this paper.

REFERENCES

Black, L. P. 1984. U–Pb zircon ages and a revised chronology for the Tennant Creek Inlier, N.T. *Aust. J. Earth Sci.* **31**, 123–131.

Black, L. P., Shaw, R. D. & Offe, L. A. 1980. The age of the Stewart Dyke swarm and its bearing on the onset of late Precambrian sedimentation in central Australia. *J. geol. Soc. Aust.* **27**, 151–155.

Black, L. P., Shaw, R. D. & Stewart, A. J. 1983. Rb–Sr geochronology of Proterozoic events in the Arunter Inlier, central Australia. *Bur. Miner. Resour. J. Aust. Geol. Geophys.* **8**, 129–138.

Clarke, G. L., Guiraud, M., Powell, R. & Burg, J.-P. 1987. Metamorphism in the Olary Block, S.A.: compression with cooling in a Proterozoic foldbelt. *J. metamorph. Geol.* **5**, 289–305.

Clarke, G. L., Collins, W. J. & Vernon, R. H. 1990. Successive Early Proterozoic metamorphism in the Anmatjira Range, central Australia. *J. metamorph. Geol.* **8**, 65–88.

Collins, W. J. & Teyssier, C. 1989. Crustal-scale ductile fault systems in the Arunta Inlier, central Australia. *Tectonophysics* **158**, 49–66.

Collins, W. J., Vernon, R. H. & Clarke, G. L. In press. Two terranes of contrasting structural evolution in the Anmatjira Range, central Australia. *J. Struct. Geol.*

England, P. C. & Richardson, S. W. 1977. The influence of erosion upon the mineral facies of rocks from different metamorphic environments. *J. geol. Soc. Lond.* **134**, 201–213.

England, P. C. & Thompson, A. B. 1984. Pressure–temperature–time paths of regional metamorphism I. Heat transfer during the evolution of regions of thickened continental crust. *J. Petrol.* **25**, 894–928.

Fry, N. 1979. Random point distributions and strain measurements in rocks. *Tectonophysics* **60**, 89–105.

Hobbs, B. E., Means, W. D. & Williams, P. F. 1976. *An Outline of Structural Geology*. John Wiley, New York.

Lindsay, J. F., Korsch, R. J. & Wilford, J. R. 1987. Timing the breakup of a Proterozoic supercontinent: evidence from Australian intracratonic basins. *Geology* **15**, 1061–1064.

Lisle, R. J. 1985. *Geological Strain Analysis, A Manual for the R_f/ϕ Technique*. Pergamon Press, Oxford.

Page, R. W. 1988. Geochronology of the early to middle Proterozoic

folds belts in northern Australia: a review. *Precambrian Res.* **40/41**, 1–19.

Platt, J. P. & Vissers, R. L. M. 1980. Extensional structures in anisotropic rocks. *J. Struct. Geol.* **2**, 387–410.

Pearson, P. J. 1988. The structural and tectonic development of the Wonga Belt and surrounding Mary Kathleen foldbelt, Mt Isa Inlier, NW Queensland. Unpublished Ph.D. thesis, University of Queensland, Brisbane, Australia.

Ramsay, J. G. 1967. *Folding and Fracturing of Rocks*. McGraw-Hill, New York.

Ramsay, J. G. & Huber, M. I. 1983. *The Techniques of Modern Structural Geology, Volume* 1: *Strain Analysis*. Academic Press, London.

Sandiford, M. & Powell, R. 1986. Deep crustal metamorphism during continental extension: moldern and ancient examples. *Earth Planet. Sci. Lett.* **79**, 151–158.

Shaw, R. D. & Langworthy, A. P. 1984. Strangways Range region. *Aust. Bur. Miner. Resour. Geol. Geophys.* 1:100,000 Geological Map Series, Canberra.

Shaw, R. D. & Stewart, A. J. 1975. Towards a stratigraphy of the Arunta Block. *Geol. Soc. Aust. Abs.* **1**, 35.

Shaw, R. D., Stewart, A. J. & Black, L. P. 1984a. The Arunta Inlier: a complex ensialic mobile belt in central Australia. Part 2: tectonic history. *Aust. J. Earth Sci.* **31**, 457–484.

Shaw, R. D., Stewart, A. J. & Rickard, M. J. 1984b. Arltunga–Harts range region. *Aust. Bur. Miner. Resour. Geol. Geophys.* 1:100,000 Geological Map Series, Canberra.

Simpson, C. & Schmid, S. M. 1983. An evaluation of criteria to deduce the sense of movement in sheared rocks. *Bull geol. Soc. Am.* **94**, 1281–1288.

Stewart, A. J. 1981. Reynolds Range region. *Aust. Bur. Miner. Resour. Geol. Geophys.* 1:100,000 Geological Map Series, Canberra.

Stewart, A. J., Offe, L. A., Glikson, A. J., Warren, R. G. & Black, L. P. 1980. Geology of the northern Arunta Block, Northern Territory. *Aust. Bur. Miner. Resour. Geol. Geophys. Rec.* 1980/83.

Vernon, R. H., Clarke, C. L. & Collins, W. J. 1989. Local, mid-crustal granulite facies metamorphism and melting: an example in the Mt Stafford area, central Australia. In: *High Pressure Metamorphism and Crustal Anatexis* (edited by Ashworth, J. R. & Brown, M.). *Spec. Publs Miner. Soc.*

Warren, R. G. 1983. Metamorphic and tectonic evolution of granulites, Arunta Block, central Australia. *Nature* **305**, 300–303.

Warren, R. G. & Stewart, A. J. 1988. Isobaric cooling of Proterozoic high-temperature metamorphites in the northern Arunta Block, central Australia. *Precambrian Res.* **40/41**, 175–198.

Wernicke, B. & Burchfield, B. C. 1982. Modes of extensional tectonics. *J. Struct. Geol.* **4**, 105–115.